JOURNAL OF CATALYSIS **173,** 64–73 (1998)
ARTICLE NO. CA971885

Synthesis of New Fe–Co Based Metal/Oxide Composite Materials: Application to the Fischer–Tropsch Synthesis

C. Cabet, A. C. Roger, A. Kiennemann, S. Läkamp,* and G. Pourroy*

*LERCSI URA CNRS 1498, 1, rue Blaise Pascal, 67008 Strasbourg, France; and *IPCMS UMR CNRS 046, 23, rue du Loess, 67037 Strasbourg, France*

Received February 21, 1997; revised July 17, 1997; accepted August 12, 1997

An original synthesis of cobalt–iron alloy/cobalt doped magnetite catalysts (spinel structure) has been developed, in which cobalt and iron are obtained in the metallic state without any reducing treatment. The chemical phenomena occurring during the preparation, based upon the coprecipitation of the hydroxides in a boiling basic medium, are detailed. By heating under argon, the composition of the metallic phase can be controlled within the range ($Co^0_{0.8}Fe^0_{0.2}$) to ($Co^0_{0.95}Fe^0_{0.05}$). X-ray diffraction, thermogravimetric analyses, and X-ray photoelectron spectroscopy experiments lead to the characterization of the crystalline phases and their location in the bulk and at the surface of the catalysts. The catalytic behavior of these composites in the hydrogenation of carbon monoxide is studied. No reducing treatment is necessary for them to be active for the Fischer–Tropsch synthesis. Moreover, an efficient treatment for protecting the spinel phase against reduction and subsequent carburization is established. The ability of such catalysts to produce C_2–C_4 olefins is also discussed.

INTRODUCTION

The Fischer–Tropsch catalysts which produce hydrocarbons from syngas are highly diversified in their formulation as are the conditions under which they are used. However, the metals readily available for obtaining industrially higher hydrocarbons on an industrial scale are mainly restricted to iron and cobalt, and, to a lesser extent, to ruthenium and nickel. The catalytic formulations have been developed in two ways: for the obtention of chemical families of products (paraffins, olefins, alcohols) or narrow distributions in one given family (C_2–C_4 olefins, gasoline, diesel, waxes. . .).

Due to the thermodynamic and kinetic limitations of the reaction, few catalysts are able to amplify the C_2–C_4 hydrocarbons fraction. However, some examples are reported in the literature and these are Fe and/or Co based catalysts on partially reductible oxide supports such as MnO_2, V_2O_5, and TiO_2 instead of the conventional inert supports like SiO_2 or Al_2O_3 (1–4). In view of producing C_2–C_4 olefins, the Fe–Mn and Co–Mn catalysts, with or without alkaline promoters, are the most studied (5–7). For these catalysts, a strong metal–manganese oxide interaction has been proposed as well as the existence of metal–Mn solid solutions at different steps of the preparation and more particularly in the case of iron on a freshly reduced catalyst (8–11). The high selectivity of C_2–C_4 has been correlated to the presence of a solid solution (12), in Fe–Mn catalysts which, for iron rich examples, was a mixed spinel phase $(Fe_{1-y}Mn_y)_3O_4$ accompanied by two carbide phases (13). For manganese rich systems, Butt (13) proposed two spinel phases, one abundant in iron $Fe_{3-y}Mn_yO_4$, the other rich in manganese β-$(Fe_{1-x}Mn_x)_2O_3$, two carbide phases (ε'-$Fe_{2.2}C$ and λ-Fe_5C_2), and the wustite phase. Unfortunately, in such catalysts, the carbide phase formed during the reaction has a short lifetime, which therefore hinders their industrial development. Cobalt does not carburize as readily as iron in presence of CO/H_2 and numerous studies have confirmed its efficiency for the obtention of light olefins (4, 14–16). As for iron based catalysts, the cobalt–manganese solid solution is essential. A catalyst where the Co : Mn atomic ratio is 1 : 1 is mainly composed of a M_3O_4 spinel in which the M cations (Co and Mn) were statistically distributed between the tetrahedral and octahedral sites. After reduction, two phases were detected: MnO and metallic cobalt. At 220°C, under CO/H_2 flow, a body centered cubic (bcc) cobalt phase was reported to be present (17, 18).

From the studies discussing the synthesis of light olefins, the following point arises: the spinel structure plays a prominent part in the preparation step. In the case of iron based catalysts, under the reaction conditions, the spinel is only partially destroyed but free Fe readily carburizes and the catalytic activity is then reduced. In the case of cobalt based catalysts the carbide formation is avoided. However, the catalysts are not active in the spinel form but as metal dispersed on partially reduced oxide matrix.

The aim of this work was to combine the respective advantages of iron and cobalt based catalysts, i.e., no destruction of the spinel structure and presence of a metal dispersed on this spinel without formation of metallic carbides. The synthesis, the characterization, and the activity in syngas reaction of Co metal/Fe–Co spinel catalysts are described. The preparative method is original and leads to

0021-9517/98 $25.00

a metallic phase (composed mainly of cobalt) without any preliminary reducing treatment, as is usually the case for the catalytic activation in the CO hydrogenation.

EXPERIMENTAL

1. Preparation of the Catalysts

The synthesis of the metal–ferrite compounds, developed by A. Malats *et al.* (19–23), has been adapted to the specific requirements of catalysis, particularly to the necessity of obtaining adequate specific surface areas. This synthesis relies upon the coprecipitation of hydroxides from cobaltous and ferrous chlorides in boiling concentrated KOH solution. Potassium hydroxide is preferred to sodium hydroxide because the solubility of KCl, formed during the synthesis, in hot water is greater than that of NaCl, which renders the washing of the catalyst much easier. Furthermore, the ionic radius of K^+ (1.33 Å) is larger than that of Na^+ (0.97 Å) and avoids the possibility of cationic insertions. The respective variation of KOH concentration and of the Co/Fe atomic ratio can lead to a wide range of compositions and properties for the metal–ferrite compounds. In the example discussed below, the Co/Fe atomic ratio equals 1/3 while the potassium hydroxide concentration is 2 mol liter^{-1}.

$CoCl_2 \cdot 6H_2O$ (4.02 g) (ACROS) and 10.08 g of $FeCl_2 \cdot 4H_2O$ (ACROS) were dissolved in 28 ml of water at ambient temperature, in order to obtain a solution where [Co + Fe] = 2 mol liter^{-1} (crystallization of water molecules being taken into account). This solution was then added with stirring to 150 ml of boiling potassium hydroxide solution ([KOH] = 2 mol liter^{-1}) obtained by dissolution of 19.7 g of KOH (BDH Anala R) in 148 ml of water. A black powder is precipitated. In one case (drying method), the precipitate was dried by total evaporation of water during 1 h with a final temperature attained of 152°C. In the second case (reflux method), the precipitate was matured by reflux at 124°C for 1 h in the boiling solution. The resulting powders from drying and reflux methods were then filtered and washed with hot water until the filtrate was neutral and was presumed to contain no chloride ions (negative $AgNO_3$ test). The precipitates were then dried at 40°C for 2 h. Fine black powders were obtained. Accordingly, the material obtained from the drying method is labeled "dried" catalyst and that from reflux method "refluxed" catalyst. The preparation routes are summarized in Fig. 1. Both precipitates were heated for 10 h under argon at 415°C and labeled, respectively, treated "dried" and treated "refluxed" catalyst. Where necessary (see Results and Discussion Section 3.1), the treated dried catalyst was submitted to various reducing treatments. It was heated under 10% H_2/He from 20 to 220°C (slope 0.2°C min^{-1}) and maintained under these conditions for either 0, 4, or 8 h.

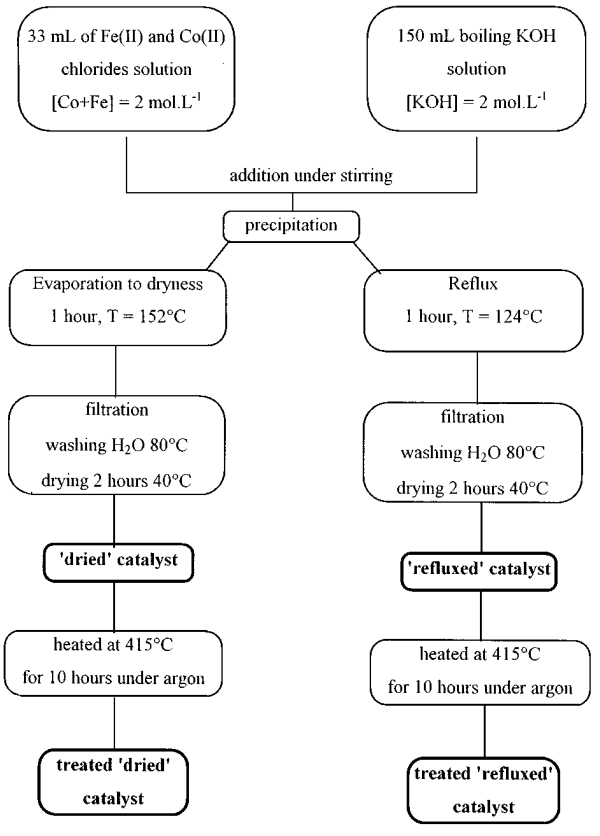

FIG. 1. Synthetic scheme for metal–ferrite compounds.

2. Characterization of the Catalysts

The samples were studied by X-ray diffraction (XRD). Data were collected at room temperature using a D5000 Siemens diffractometer equiped with a primary beam quartz monochromator (Co $K\alpha_1 = 1.78897$ Å).

The specific surface areas of the catalysts were measured by the BET method based on the N_2 physisorption capacity at 77 K. The values are summarized in Table 1.

The Co/Fe ratios were determined by atomic absorption at the Service Central d'Analyse du CNRS (Vernaison, France) and by energy dispersive X-ray analysis. The morphology of these materials were observed by scanning electron microscopy (SEM) on a JEOL 840 apparatus.

Thermal gravimetric and thermal differential analyses (TGA–TDA) were carried out in alumina crucibles under atmospheres of nitrogen and air, using a SETARAM 92-12 apparatus.

The surfaces of the samples were examined by X-ray photoelectron spectroscopy (XPS) on a VG-ESCA 3 apparatus. Binding energies were calibrated with respect to the signal for adventitious carbon (binding energy = 284.8 eV).

3. Reactivity in the CO Hydrogenation

3.1. CO disproportionation. Catalyst (0.1 g) was heated under helium (20 liters h^{-1} g_{cat}^{-1}) at 220°C (1°C min^{-1}). Pulses

TABLE 1

Specific Areas of the Fe–Co Catalysts

Catalyst and treatment		Specific surface area ($m^2\ g_{cat}^{-1}$)
Dried catalyst	Fresh	28
Treated dried catalyst	Fresh	20
	Heated at 200°C under 10% H_2/He	12
	Heated and maintained 4 h at 200°C under 10% H_2/He	13
	Heated and maintained 8 h at 200°C under 10% H_2/He	13
	After CO/H_2 reaction	<1
Refluxed catalyst	Fresh	13
Treated refluxed catalyst	Fresh	8
	After CO/H_2 reaction	2

Note. Dried catalyst, treated dried catalyst, refluxed catalyst, and treated refluxed catalyst are prepared according to Fig. 1.

of carbon monoxide (0.5 ml) were admitted onto the catalyst at steady intervals (8 min), using a six-port switching valve. This process was repeated until a stabilization of the amount of CO_2 formed was observed. The exit gases (CO and CO_2) were analyzed by gas chromatography.

When necessary, the reducing treatments were performed *in situ* under 10% H_2/He (total gas flow: 30 liters $h^{-1}\ g_{cat}^{-1}$).

3.2. Catalytic tests. Catalytic tests were carried out in a fixed bed reactor. The feed gas flow rate was adjusted by mass flow controller. The pressure was regulated by coupling a pressure comparator and an electronic control valve.

For no reducing treatment, the catalyst (300 mg) was heated to 200°C (0.2°C min^{-1}) under nitrogen (2.3 liters h^{-1} at 1 MPa). Then, the nitrogen was replaced by the CO/H_2 mixture ($CO/H_2 = 1$, total flow gas = 0.5 liter h^{-1}, GHSV = 2000 h^{-1}, $P = 1$ MPa) and the temperature increased to 220°C.

The catalysts were also tested under their reduced form. The reducing treatment was performed *in situ* at 1 MPa under a 10% H_2/N_2 (total flow gas 2.6 liters h^{-1}) from 20 to 200°C (0.2°C min^{-1}). At 200°C, the gases were substituted by the CO/H_2 mixture and the temperature was further increased. For each temperature, on one side, the catalytic results are given at the steady state after a stabilization of almost 50 h, on the other side, the catalyst is maintained 120 h while the analyses are performed at regular intervals.

The exit gases were analyzed by on-line gas chromatography. Liquid products were regularly collected from a cooled trap and analyzed by chromatography.

The CO conversion (%), the molar selectivities (%) and the hydrocarbon distributions (wt%) were calculated as follows:

$$\text{CO conversion (\%)} = 100 \times \frac{\text{moles of transformed CO}}{\text{moles of initial CO}}$$

$$\text{selectivity to products (\%)} = 100 \times \frac{\text{CO moles transformed into the given product}}{\text{total transformed CO moles}}$$

$$\text{selectivity to } C_i \text{ (wt\%)} = 100 \times \frac{\text{mass of } C_i}{\text{total mass of hydrocarbons}}.$$

RESULTS AND DISCUSSION

1. Characterization of Dried and Refluxed Catalysts

1.1. X-ray diffraction. The diffraction diagrams of dried and refluxed catalysts are shown in Fig. 2. The compounds are highly crystallized (narrow diffraction peaks and low background). At room temperature, they are made of two phases, a spinel phase (named s) and a metallic phase isomorphous to α-Fe having a bcc structure (named b). The lattice parameter of the spinel is $a = 8.402(5)$ Å. The corresponding value, $a = 2.838(5)$ Å, for the metallic phase indicated that the bcc phase is an iron–cobalt alloy containing about 20% of Fe (24). Thus, the dried and refluxed catalysts can be formulated as $(Co^0_{0.8}Fe^0_{0.2})_\beta\,[Co_xFe_yO_4]$. In both cases, a high background in the low angles region revealed the presence of an amorphous phase, possibly hydroxides; it is more pronounced for the dried catalyst.

1.2. Elemental analysis—energy dispersive X-ray analysis. The Co/Fe atomic ratios determined by elemental analysis are consistent with those determined by energy dispersive X-ray analysis. The values obtained for the dried and refluxed catalysts are 0.42 and 0.40, respectively. For the treated dried and treated refluxed catalyst, they are 0.43 and 0.40, respectively. The Co/Fe ratios remain unchanged during the thermal treatment. However, all of the ratios are

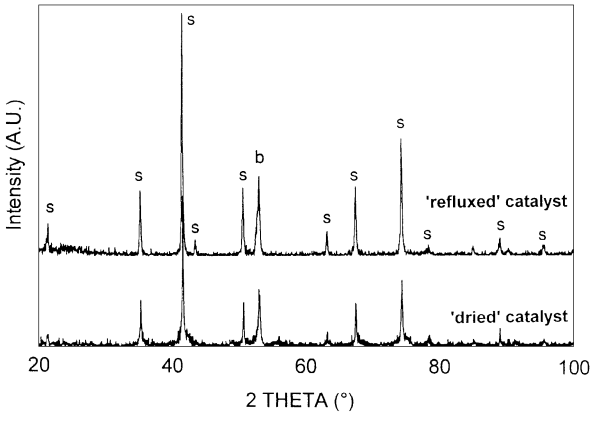

FIG. 2. X-ray diffraction patterns of the dried catalyst and the refluxed catalyst prepared according to Fig. 1. s and b refer to spinel and Fe–Co alloy, respectively.

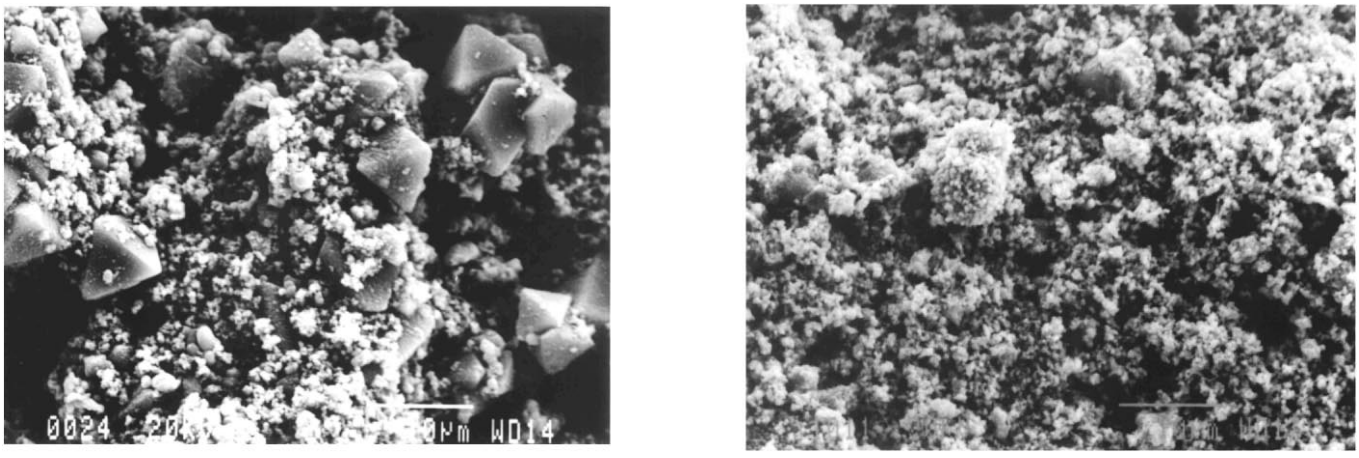

FIG. 3. Scanning electron micrographs (SEM) of the dried catalyst (left) and the refluxed catalyst (right) prepared according to Fig. 1.

found to be higher than the expected value of 0.33, that of the starting solution. The values of Co/Fe ratio indicate that some iron is lost during the preparation. Neither chlorine nor potassium were detected in the bulk.

1.3. Scanning electron microscopy. The examination of dried and refluxed catalysts (see Fig. 3) revealed structural differences which are probably due to the maturation in boiling KOH. The dried catalyst comprised large grains of octahedral shape, having sides of almost 8 μm. These large grains are embedded in a matrix consisting of small grains. The refluxed catalyst is composed of small grains (100–300 nm) which exhibited no defined geometry. Thus, the former appeared more heterogeneous in terms of its morphology. During the preparation, it was matured by evaporation to dryness while the latter was matured in boiling medium, which might explain why in the case of dried catalyst, grain growth occurred in preferential sites.

1.4. TGA–TDA analyses. To quantify the amorphous phase, thermal gravimetric analyses were performed under inert gas (nitrogen) between 20 and 900°C (slope 5°C min^{-1}). They are presented in Fig. 4a. For the dried catalyst, the weight loss between 150 and 600°C, attributable to the decomposition of the amorphous hydroxide phase detected by XRD, is 2.71%. In the case of the refluxed catalyst, the corresponding weight loss is only 0.77% and confirms that it contains less amorphous phase than the dried catalyst.

The diffraction pattern of this latter following the above thermal gravimetric analysis, indicated the presence of cobalt doped magnetite spinel, a cobalt fcc phase (f) and traces of cobalt oxide CoO. The presence of this oxide would suggest that the hydroxide amorphous phase, initially present in the dried catalyst, is mainly cobalt hydroxide.

A gravimetric analysis in air allows to precise their formula. Indeed, from the mass increase due to oxidation, β, x, and y of the formula $(Co^0_{0.8}Fe^0_{0.2})\beta$ $[Co_xFe_yO_4]$ can be

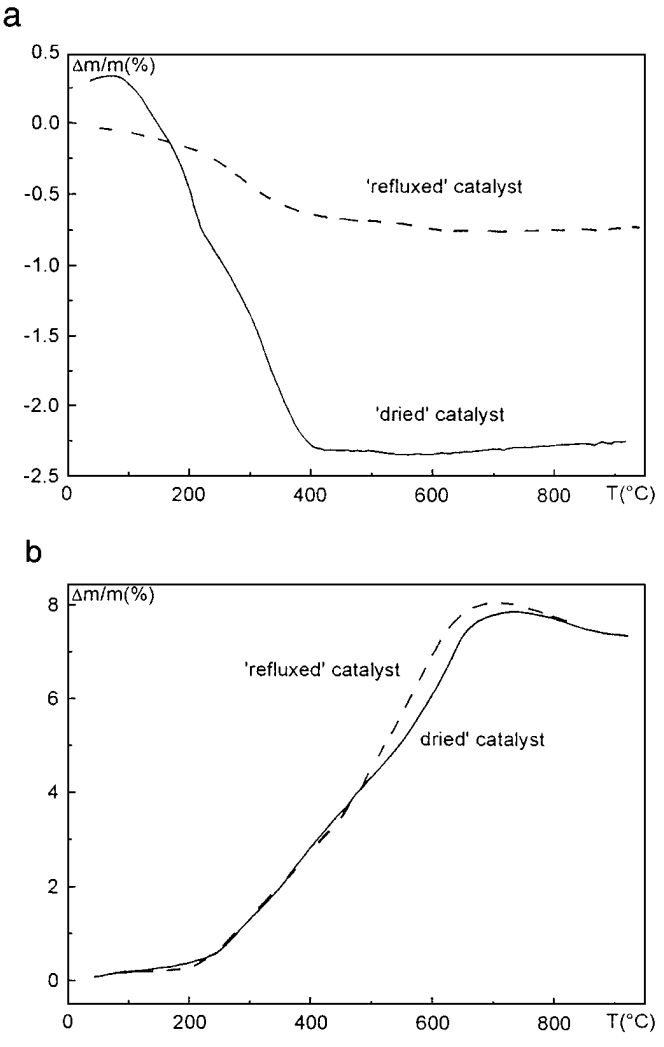

FIG. 4. Thermal gravimetric analysis (TGA) of the dried catalyst (—) and the refluxed catalyst (- -) prepared according to Fig. 1(a) under nitrogen and (b) under air.

determined. The presence of an amorphous phase prevents any precise formulation. However, approximations could be made. For the dried catalyst, the weight increase due to oxidation is 7.24% (Fig. 4b), while that due to the hydroxide decomposition is 2.71%, giving a value of 7.44% for the mass increase corrected with respect to the presence of hydroxides. The elemental analysis gave Co/Fe = 0.42, this corresponds to a global composition of $CoFe_{2.38}O_p$. The mass increase leads to the value of $p = 3.42$, so the global compound can be formulated as $Co_{1.17}Fe_{2.78}O_4$. XRD suggested that the compound corresponds to $(Co^0_{0.8}Fe^0_{0.2})_\beta$ $[Fe_xCo_yO_4]$. The identification of the parameters β, x, and y leads now to the formula $(Co^0_{0.8}Fe^0_{0.2})_{0.95}$ $[Fe_{2.66}Co_{0.34}O_4]$ for the dried catalyst. In the case of the refluxed catalyst, the corrected weight increase due to oxidation is 7.46% (Fig. 4b) and the weight loss due to the hydroxide decomposition is 0.77%. The calculated formula is $(Co^0_{0.8}Fe^0_{0.2})_{0.93}$ $[Fe_{2.62}Co_{0.38}O_4]$. Due to the presence of an amorphous phase, it must be noted that these formulations are approximative.

The synthesis of these catalysts is believed to be based upon several steps as follows:

—the coprecipitation in boiling concentrated basic medium of a cobalt iron mixed hydroxide (from the corresponding chlorides),

$$x\,CoCl_2 \cdot 6H_2O + y\,FeCl_2 \cdot 4H_2O \xrightarrow{\text{conc. KOH}} Co_xFe_y(OH)_{2(x+y)} + 2(x+y)KCl;$$

—the dehydration of the hydroxide to an oxide in alkaline medium,

$$Co_xFe_y(OH)_{2(x+y)} \xrightarrow{OH^-} Co_xFe_yO_{x+y} + (x+y)H_2O.$$

The formation of the metallic phase of the catalysts can now be explained. Indeed, according to the literature, FeO is known to disproportionate below 570°C (25):

$$4FeO \rightarrow Fe_3O_4 + Fe^0 \quad (\Delta G^\circ_{25} = -9.8 \text{ kcal}).$$

However, the same phenomenon was reported for precipitates or gels of $Fe(OH)_2$ (26–28) according to

$$4Fe(OH)_2 \rightarrow Fe_3O_4 + Fe^0 + 4H_2O \quad (\Delta G^\circ_{25} = -7.7 \text{ kcal}).$$

In our case, disproportionation from the mixed hydroxide $Co_xFe_y(OH)_{2(x+y)}$ or from the mixed oxide $Co_xFe_yO_{x+y}$ is possible. In both cases there is significant formation of Fe^0. Then the following redox reaction occurs to form Co^0:

$$Co^{2+} + Fe^0 \rightarrow Co^0 + Fe^{2+} \qquad E^\circ(Fe^{2+}/Fe) = -0.409 \text{ V}$$
$$E^\circ(Co^{2+}/Co) = -0.28 \text{ V}.$$

The reduction of Co^{2+} into Co^0 is favored, which would explain why the alloy obtained is rich in Co ($\sim$80% at Co).

It must be noted that the β value is close to 1.0, the highest possible value. Indeed, the metallic phase results from the disproportionation of Fe(II) according to the reactions given above, thus the total amount of (Co + Fe) metallic can not exceed a third of (Co + Fe) in the spinel.

To summarize, the dried and refluxed catalysts are close to identical in their composition. The differences between the compounds lie in their specific surface areas (respectively 28 and 13 $m^2\,g^{-1}$), in their morphological aspect and in the amount of amorphous phase (probably cobalt rich hydroxides) they contain. These differences can be attributed to the methods of maturation during their preparation.

2. *Characterization of Treated "Dried" and "Refluxed" Catalysts*

The structural evolution during heating under argon is shown in the XRD patterns displayed in Fig. 5. From 300°C, the intensity of diffraction peaks of the cobalt–iron bcc alloy (b) decreased in favor of the cobalt fcc phase (f). At 415°C only the fcc phase is present. According to the Fe–Co phase diagram (24), this means that under heating the alloy

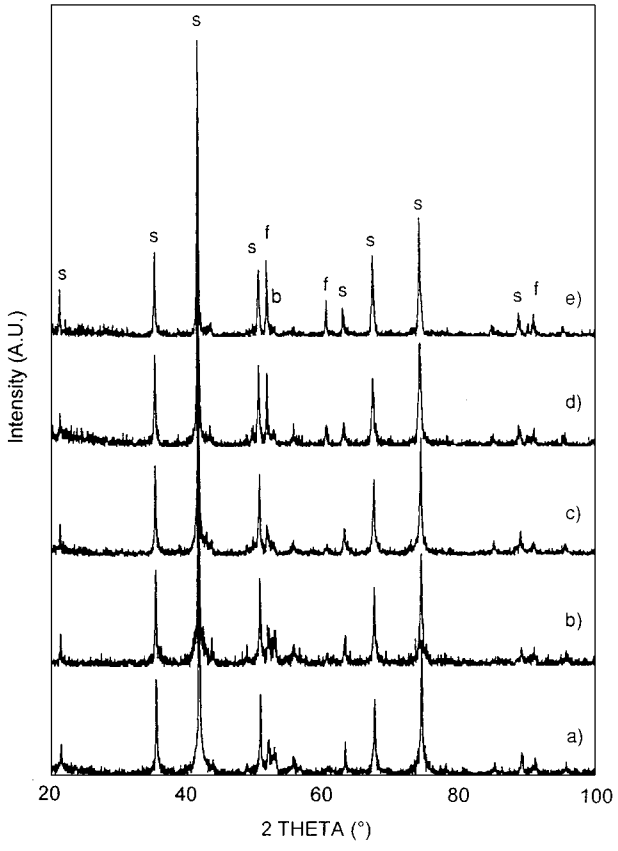

FIG. 5. Evolution of the X-ray diffraction pattern of the dried catalyst prepared according to Fig. 1, during heating under argon at (a) 300°C, (b) 350°C, (c) 370°C, (d) 400°C, (e) 415°C. s, b, and f refer to the spinel phase, the alloy of bcc structure, and the alloy of fcc structure, respectively.

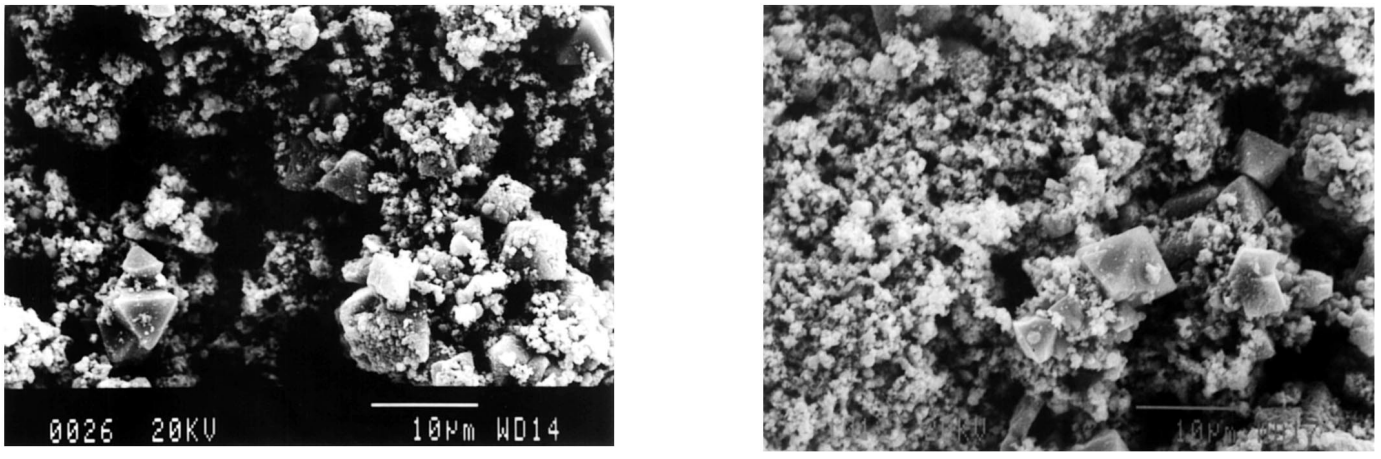

FIG. 6. Scanning electron micrographs (SEM) of treated dried catalyst (left) and treated refluxed (right) catalyst prepared according to Fig. 1.

was reduced in iron content while simultaneously being enriched in cobalt. The lattice parameter of 3.550(5) Å observed for the fcc phase corresponds to a composition of the alloy of the treated dried catalyst of $Co^0_{0.95}Fe^0_{0.05}$. The spinel phase is conserved and the lattice parameter of $a = 8.394(5)$ Å remains almost unchanged.

The evolution of the refluxed catalyst is identical and the X-ray diffraction diagrams of treated dried and treated refluxed catalysts were equally similar.

Thermal gravimetric analyses under argon were performed on the treated dried and treated refluxed catalysts. The respective weight losses were only 0.25 and 0.21% (compared to 2.71 and 0.77% for the nontreated samples). This indicates that the hydroxides initially present decompose by heating at 415°C. In air, the weight increases were, respectively, 6.68 and 6.22%. The calculated formula of the treated dried catalyst is $(Co^0_{0.95}Fe^0_{0.05})_{0.82}$ $[Fe_{2.65}Co_{0.35}O_4]$; that of the treated refluxed catalyst is $(Co^0_{0.95}Fe^0_{0.05})_{0.74}$ $[Fe_{2.63}Co_{0.37}O_4]$. These were consistent with the fact that the spinels remained almost unchanged by heating under argon.

In contrast, heating under argon at 415°C led to partial breaking down of the metallic phase (β equals 0.82 for the treated dried catalyst and 0.74 for the treated refluxed catalyst, respectively, compared to 0.95 for the dried catalyst and 0.93 for the refluxed catalyst). The decomposition of the hydroxides of the nontreated samples is thought to be responsible for the partial oxidation of the compounds. If no hydroxides remained in the nontreated samples, the amount of metallic part would be conserved under heating.

Under heating, the composition of the two phases was changed. The metallic alloy was enriched in cobalt while the spinel was enriched in iron according to

$$Fe^0 + Co^{II}_{spinel} \xrightarrow[415°C]{Ar} Fe^{II}_{spinel} + Co^0.$$

The treated dried and treated refluxed catalyst can be considered as metallic cobalt over cobalt doped magnetite: almost 17 wt% Co^0/spinel in both cases. This amount of metallic cobalt proved consistent with the concentration range usually used in the Fischer–Tropsch synthesis (29). Once more, as for the nontreated samples, the formulations of the treated dried and treated refluxed catalyst proved almost identical. The differences of the specific surface areas encountered for the nontreated samples were conserved since for the treated dried and treated refluxed catalysts these values were, respectively, 20 and 8 $m^2\ g^{-1}_{cat}$.

They were also studied by scanning electron microscopy (Fig. 6). The treated dried catalyst is very similar to the respective nontreated sample. The treated refluxed catalyst, unlike the nontreated sample, exhibited some grains of octahedral shape. The crystallization of the amorphous phase during heating at 415°C revealed by XRD and subsequent thermal gravimetric analysis was accompanied by microstructural alteration.

Surface studies were carried out by XPS. The surface atomic ratios were calculated. For the dried catalyst, the surface atomic Co/Fe ratio is higher (0.5) than the Co/Fe bulk ratio (0.42), indicating that at the surface the amount of Co is higher than in the bulk. If it is considered that the phases present at the surface are the same as those in the bulk (alloy $Co^0_{0.8}Fe^0_{0.2}$ and spinel $Fe_{2.59}Co_{0.41}O_4$), this would mean that the surface of the dried catalyst is enriched in alloy with respect to the bulk. However, since no metallic element is detected by XPS, then Co^0 and Fe^0 are not included in the surface Co/Fe ratio of 0.51. That cobalt rich hydroxides are present at the surface of the dried catalyst must be considered and equally that they shield metallic cobalt, consequently protecting this layer from oxidation. This is consistent with the fact that hydroxides were detected by XRD and thermal gravimetric analyses.

The case of the refluxed catalyst is very similar. The Co/Fe surface ratio is 0.84. No metallic element was detected.

However, despite the high value of Co/Fe ratio at the surface, the thermally treated sample did not contain as many hydroxides as the dried catalyst. Therefore, in addition to a cobalt rich hydroxide phase, a cobalt oxide phase has to be considered.

For the treated dried and treated refluxed catalysts, the calculation of the phase distribution at the surface is allowed since these compounds have been shown to be free of hydroxides. This time the two phases are $Co^0_{0.95}Fe^0_{0.05}$ and $Fe_{2.65}Co_{0.35}O_4$ (or $Fe_{2.63}Co_{0.37}O_4$ for the treated refluxed catalyst). The Co/Fe surface ratio of the treated dried catalyst is 0.31 (lower than the bulk ratio). Metallic Co is detected: the alloy (poor in Fe) is present at the surface (and Fe^0 is not detected). The calculation leads to the formula $(Co^0_{0.95}Fe^0_{0.05})_{0.50}$ $[Fe_{2.65}Co_{0.35}O_4]$ for the surface of the treated dried catalyst. When compared with the bulk formula (where $\beta = 0.82$), the surface of the treated dried catalyst was enriched in oxide phase (spinel) while the part of the metallic phase is reduced. The same reasoning for the treated refluxed catalyst for which Co/Fe surface ratio is 0.44, gives $(Co^0_{0.95}Fe^0_{0.05})_{0.85}$ $[Fe_{2.63}Co_{0.37}O_4]$ for the surface composition. In this case the metallic content is both higher in the bulk of the treated refluxed catalyst and at the surface of the treated dried catalyst.

3. *Reactivity of the Treated Dried and Treated Refluxed Catalyst in CO Hydrogenation*

3.1. CO disproportionation. As indicated in previous works on Fe (30), Co (31, 32), or bimetallic Co–Cu (33) based catalysts, the carbon monoxide disproportionation reaction,

$$2CO \rightarrow C_{surface} + CO_2,$$

is a means of simulating the first step of the mechanism of the Fischer–Tropsch synthesis, which can also be useful for comparing catalytic activities and here provides the means by which CO disproportionation on the treated dried and treated refluxed catalyst under various conditions was studied.

Figure 7 presents the CO disproportionation curves at 220°C for the treated dried and treated refluxed catalysts, and at 240 and 260°C for the treated dried catalyst. Figure 8 relates the effect of the reduction (see experimental section) on the disproportionation activity of this latter at 220°C.

From Fig. 7, at 220°C, the treated dried catalyst (20 $m^2\ g^{-1}_{cat}$) would seem to be slightly more active than the treated refluxed catalyst (8 $m^2\ g^{-1}$). An increase in disproportionation temperature induces higher activity. Figure 8 reveals that the reduction of the treated dried catalyst has no effect upon the disproportionation activity (except for an 8-h reduction treatment). This phenomenon is surprising for conventional Fischer–Tropsch catalysts but understandable in our case since the treated dried catalyst already possesses a metallic phase able to dissociate CO; thus reduction is not necessary to produce metallic sites. The lower activity of the reduced catalysts compared to that of the treated dried catalyst can be explained by the decrease of the specific surface area following reduction (13 $m^2\ g^{-1}$ instead of 20 $m^2\ g^{-1}$). A more profound reduction of 8 h induced an increase of the disproportionation activity, while the specific surface area remained stable. In this case, it can be suggested that the reduction generated metallic sites, active for the disproportionation of carbon monoxide. This is not necessarily a favorable phenomenon since the active sites can be induced only by the spinel reduction. The sites for iron metal thus generated can easily carburize to the detriment of the catalytic activity. Further, the diffraction diagrams of the treated dried catalyst after an 8-h reduction treatment or not are similar but for $d = 2.01$–2.02 Å a peak is present for the reduced catalyst. This peak signifies the presence of an iron rich metallic phase. The SEM examination reveals a breaking of the octahedral grains (see Fig. 9).

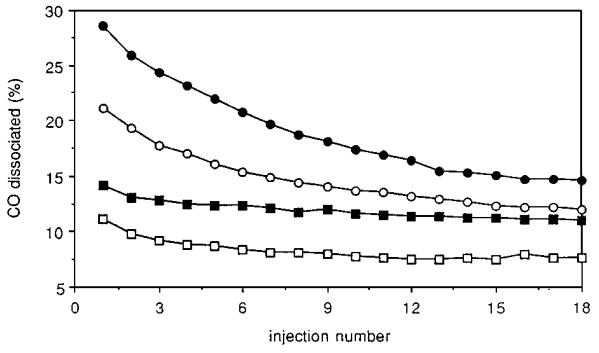

FIG. 7. Disproportionation curves of treated dried catalyst and treated refluxed catalyst prepared according to Fig. 1 at various temperatures. (■) Treated dried catalyst at 220°C, (○) treated dried catalyst at 240°C, (●) treated dried catalyst at 260°C, (□) treated refluxed catalyst at 220°C.

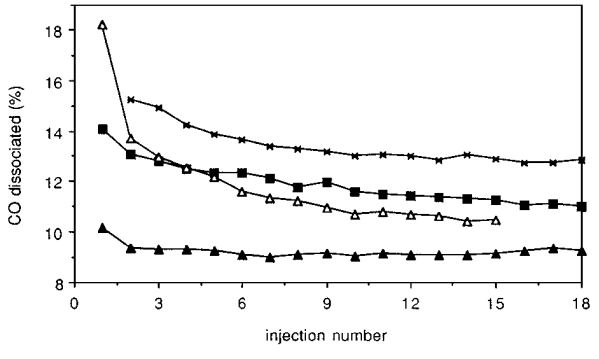

FIG. 8. Disproportionation curves of treated dried catalyst prepared according to Fig. 1, at 220°C after various reducing treatments: (■) fresh, (▲) heated at 220°C under 10% H_2/He, (△) maintained 4 h at 220°C under 10% H_2/He, (×) maintained 8 h at 220°C under 10% H_2/He.

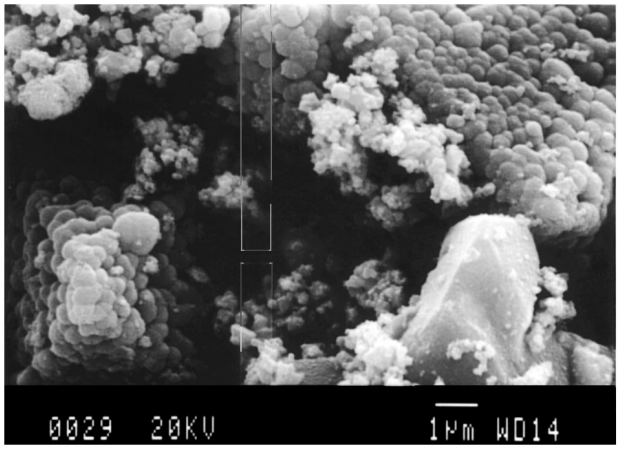

FIG. 9. Scanning electron micrograph (SEM) of treated dried catalyst prepared according to Fig. 1 after an 8-h reducing treatment at 220°C under 10% H_2/He.

3.2. Catalytic tests. The treated dried and treated refluxed catalyst were studied in the carbon monoxide hydrogenation reaction for their capacity to produce C_2–C_4 olefins.

First, the catalysts were studied in their reduced form (see Experimental). Then, they were tested without prior reducing treatment and the CO/H_2 mixture was introduced at 200°C under 1 MPa (see Experimental).

The catalytic results obtained are summarized in Table 2.

The total CO conversions are consistent with the results obtained by the carbon monoxide disproportionation experiments. Indeed, in the case of the treated dried catalyst, the reduced catalyst is less active than the nonreduced one at 220°C (1.7% compared to 2.0%). At 220°C, the treated refluxed catalyst remains inactive while the treated dried catalyst converts 2.0% of CO. However, at 240 and 250°C, the former becomes more active than the latter (5.0 and 9.0% of CO conversion for the former, and 4.1 and 6.9% for the latter). As indicated in Fig. 7, with increasing temperature, the CO conversion over the treated dried catalyst increases (4.1% at 240°C and 6.9% at 250°C). This phenomenon also occurs for reduced treated dried and treated refluxed catalysts.

The molar selectivity for CO_2 was high for the treated dried catalyst and its reduced form, and reduced treated refluxed catalyst, but decreased with increasing temperature in favor of the hydrocarbon fraction: for reduced treated dried catalyst, the CO_2 selectivity decreased from 88.9 to 66.3% when the temperature was increased from 220 to 280°C, while the selectivity for hydrocarbons increased from 7.7 to 33.0%.

The treated refluxed catalyst behaved differently since selectivity for CO_2 was only 40.4% at 240°C, while that for the hydrocarbon was 56.4%. These results showed no improvement at higher temperatures. In all cases, the alcohol formation was low and alcohol selectivity never exceeded 3.4%. Notably, the higher alcohol detected was hexanol.

Concerning the hydrocarbon distribution, once again, the treated dried catalyst and its reduced form, and reduced treated refluxed catalyst, presented the same catalytic behavior. For reduced treated dried catalyst, the methane fraction was 51.1% at 220°C, which decreased to 36.0%

TABLE 2

Catalytic Results of Treated Dried Catalyst, Treated Refluxed Catalyst, and the Corresponding Reduced Catalysts at Various Temperatures ($P = 1$ MPa; $CO/H_2 = 1$; GHSV = 2000 h^{-1})

Catalyst	Reduced treated dried catalyst			Reduced treated refluxed catalyst	Treated dried catalyst			Treated refluxed catalyst	
T (°C)	220	250	280	240	220	240	250	240	250
Total CO conversion (%)	1.7	9.3	24.0	8.8	2.0	4.1	6.9	5.0	9.0
Molar selectivities (%) into									
CO_2	88.9	83.2	66.3	80.6	84.2	78.5	68.8	40.4	55.8
Hydrocarbons	7.7	16.0	33.0	18.5	15.1	20.1	30.1	56.4	41.4
R–OH($<C_6$)	3.4	0.8	0.7	0.9	0.7	1.4	1.1	3.2	2.8
Hydrocarbons distribution (wt%)									
C_1	55.1	52.7	36.0	44.2	52.9	54.1	36.1	63.3	54.9
$C_2^=$	8.8	6.9	3.4	6.4	8.7	7.8	4.9	4.9	3.9
C_2	3.8	4.9	3.6	4.8	3.3	7.9	3.2	9.8	6.5
$C_3^=$	9.6	9.1	5.0	9.6	8.7	7.9	5.9	6.8	7.6
C_3	2.4	1.8	1.0	2.2	2.2	3.6	1.1	3.3	1.6
$C_4^=$	5.2	4.9	2.5	6.9	5.3	4.5	3.3	3.7	4.2
C_4	3.6	3.5	1.0	3.2	3.5	4.1	1.4	2.6	1.5
C_5^+	11.5	16.1	47.4	22.7	15.4	10.1	44.2	5.6	19.8
Total C_2–C_4	33.4	31.1	16.5	33.1	31.7	35.8	19.8	31.1	25.3
O/P	2.4	2.0	1.9	2.2	2.5	1.3	2.5	1.0	1.6

Note. Treated dried catalyst and treated refluxed catalyst have been prepared according to Fig. 1. The reduced form has been obtained by heating the catalysts at 200°C under 10% H_2/He. O/P, olefin/paraffin ratio in C_2–C_4 fraction.

at 280°C. At this temperature, the C_2–C_4 fraction was also lowered (from 33.4 to 16.5%) in favor of the C_5^+ fraction (from 11.5 to 47.4%). Varying the temperature between 220 and 280°C induced a slight decrease of the olefin/paraffin ratio (O/P) from 2.4 to 1.9. Reduced treated refluxed catalyst, studied at 240°C, gave similar results to reduced treated dried catalyst (CH_4, 44.2%; C_2–C_4, 33.1%; C_5^+, 22.7%; and O/P = 2.2). For the treated dried catalyst at 220, 240, and 250°C, the variation in the catalytic results was identical except for the value of the O/P ratio (2.5 at 250°C). The C_2–C_4 fraction was of the order of 19.8% at 250°C with the C_5^+ fraction representing 44.2% of the hydrocarbons.

In the case of treated refluxed catalyst, the catalytic results were different. At isoconversion of CO, the selectivity toward methane was 54.9% at 250°C (compared to 52.7% for reduced treated dried catalyst at 250°C and 44.2% at 240°C for reduced treated refluxed catalyst) and the C_5^+ fraction was smaller; the C_2–C_4 fraction remained satisfactory. The chain growth probability (α), calculated in the C_2–C_6 fraction, was the value of 0.44 for the treated refluxed catalyst at 240°C, while, at the same temperature, α equals 0.53 for the treated dried catalyst. This provided confirmation that, at 240°C, the treated refluxed catalyst is more favorable to the light hydrocarbons than the treated dried catalyst. However, the most significant difference lies in CO_2 selectivity which is less than half for treated refluxed catalyst at 240°C than for the other three catalysts.

The specific surface areas of the treated dried catalyst and the treated refluxed catalyst after catalytic test were low (1 and 2 $m^2\ g_{cat}^{-1}$, respectively).

The diffraction diagrams of the four catalyst after test are presented in Fig. 10, as well as that of fresh treated refluxed catalyst. They were similar for treated dried catalyst, reduced one, and reduced treated refluxed catalyst after test. The peaks of the spinel phase are significantly decreased and a carbide phase was detected. The amount of this carbide phase increased with the duration of the catalytic test, the temperature of reaction conditions, and iron carburization.

For treated refluxed catalyst after test, the diffraction peaks of the spinel (a cobalt doped magnetite with $a =$ 8.394 (5) Å) are almost unchanged with respect to those before test. Concerning the metallic phase, a fcc cobalt phase was detected, as was, an iron rich Fe–Co alloy, as in the case of the treated dried catalyst after an 8-h reduction treatment (see Section 3.1) and a weak peak characteristic of Fe_2C. Therefore, it seems that only the metallic phase appeared to be affected by the reactivity under CO/H_2. The treated refluxed catalyst is then the only catalyst whose spinel remains stable during CO hydrogenation reaction. The other three catalysts studied reduce and carburize. These phenomena imply an explanation for the similarities of the catalytic behaviors of the treated dried catalyst, reduced one and reduced treated refluxed catalyst, while treated refluxed catalyst does not present the same catalytic results.

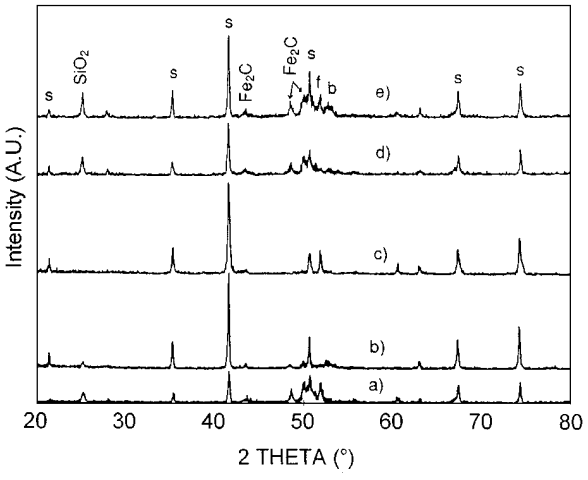

FIG. 10. X-ray diffraction patterns of (a) treated dried catalyst after catalytic test, (b) treated refluxed catalyst after catalytic test, (c) treated refluxed catalyst before catalytic test, (d) reduced treated dried catalyst after catalytic test, and (e) reduced treated refluxed catalyst after catalytic test. The samples have been prepared according to Fig. 1 and the reduced form has been obtained by heating the catalysts at 200°C under 10% H_2/He. s, b, and f refer to the spinel phase, the alloy of bcc structure, and the alloy of fcc structure, respectively.

The reduction of the spinel during the catalytic test of the reduced samples can be explained by the fact that the reduction before test partially reduced the spinel phase. Some metallic Fe sites were created. These sites were precursors to very stable iron carbides and, under the reaction conditions, in the presence of $C_{surface}$ coming from CO disproportionation displace the spinel reduction reaction according to

$$\mathrm{Co}_x\mathrm{Fe}_{3-x}\mathrm{O}_4 \rightleftharpoons \underbrace{(3-x)\mathrm{Fe}^0 + x\mathrm{Co}^0}_{\downarrow C_{surface}} \quad (x \ll 3-x, \text{ iron rich alloy})$$
$$(3-x)/2\mathrm{Fe}_2\mathrm{C} + x\mathrm{Co}^0.$$

When treated refluxed catalyst is put in contact with CO/H_2 at 200°C, the catalyst activity, though weak, generated the formation of CO_2 and H_2O. The reducing capacity of syngas is then lowered and the reduction of the spinel does not occur. For the treated dried catalyst, although treated under the same conditions, the spinel is reduced under test. In the case of the treated dried catalyst, it must be remembered that the specific surface area is higher than for treated refluxed catalyst and the surface compositions determined from XPS studies demonstrated that the surface of the treated dried catalyst was enriched in spinel ($\beta = 0.50$) with respect to that of treated refluxed catalyst ($\beta = 0.85$). In brief, that more spinel is accessible to reducing gases can explain why the treated dried catalyst is reduced

under the reaction conditions, while the treated refluxed catalyst remains unchanged.

CONCLUSION

This work presents the preparation of cobalt–iron alloy/cobalt doped magnetite catalysts in which cobalt and iron are obtained in the metallic state. By heating at 415°C under inert gas, crystallographic restructurations occur in the compounds and the metallic phase becomes mainly composed of elemental cobalt.

The methods by which the compounds were matured during preparation induced morphological differences and variations of both the specific surface areas and the metallic-oxide phases distribution at the surface which influences the spinel stability toward reduction under the reaction conditions. In fact, the greater the amount of the spinel phase at the surface of the catalyst, the more the oxide is exposed to reducing gases. Then, as soon as metallic sites are created, very stable iron carbides are formed which favor the spinel reduction.

The catalysts studied do not require any reduction step to be efficient in the Fischer–Tropsch synthesis, Further, when reducing treatments were performed before catalytic tests, the spinel phase of the compounds partially reduces and the catalysts easily carburize under the reaction conditions; this is to the detriment of the catalytic activity (high production of CO_2).

An efficient treatment for protecting the catalyst from reduction and subsequent carburization was established: the compounds were heated at 200°C under nitrogen and then the inert atmosphere is substituted with the CO/H_2 mixture. At 200°C, the catalyst activity, though weak, generated the formation of CO_2 and H_2O and lowered the reducing capacity of syngas.

When the spinel is preserved, a selectivity to hydrocarbons of 56.4% (31.1% C_2–C_4) can be obtained for a CO conversion of 5%.

ACKNOWLEDGMENT

The authors thank Mr. P. Poix for his advice concerning the synthesis of the composite materials.

REFERENCES

1. Tauster, S. J., Fung, S. C., and Garten, R. L., *J. Am. Chem. Soc.* **100**, 170 (1978).
2. Kugler, E. L., and Tauster, S. J., U.S. Patent 4,206,135 (1980) assigned to Exxon Research and Engineering Co.
3. Kugler, E. L., and Tauster, S. J., U.S. Patent 4,206,134 (1980) assigned to Exxon Research and Engineering Co.
4. Copperthwaite, R. G., Hutchings, G. J., Van der Riet, M., and Woodhouse, J. R., *Int. Eng. Chem. Res.* **26**, 969 (1987).
5. Kölbel, H., and Tillmetz, K. D., German Patent 2,507,647 (1976) U.S. Patent 4,177,203 (1976) assigned to Ruhrchemie AG.
6. Bussenmeier, B., Frohning, C. D., Horn, G., and Klug, W., German Patent 2,518,964 (1976) assigned to Ruhrchemie AG.
7. Barrault, J., Renard, C., Yu, L. T., and Gal, J., "Proceedings for the 8th International Congress on Catalysis," Vol. II, p. 101. Verlag Ed., Berlin, 1984.
8. Jaggi, N. K., Schwartz, L. H., Butt, J. B., Papp, H., and Baerns, M., *Appl. Catal.* **10**, 347 (1985).
9. Maiti, G. C., Malessa, R., and Baerns, M., *Appl. Catal.* **5**, 151 (1983).
10. Barrault, J., and Renard, C., *Appl. Catal.* **14**, 133 (1985).
11. Van Dijk, W. L., Niemantsverdriet, J. W., Van der Kraan, A. M., and Van den Baan, H. S., *Appl. Catal.* **2**, 273 (1982).
12. Hutchings, G. J., and Boeyens, J. C. A., *J. Catal.* **100**, 57 (1986).
13. Butt, J. B., *Catal. Lett.* **7**, 83 (1990).
14. Hutchings, G. J., Van der Riet, M., and Hunter, R., *J. Chem. Soc. Farad. Trans. 1* **85**, 2875 (1989).
15. Van der Riet, M., Copperthwaite, R. G., and Hutchings, G. J., *J. Chem. Soc. Farad. Trans. 1* **83**, 2963 (1987).
16. Chen, H., and Adesina, A. A., *Appl. Catal. A* **112**, 87 (1994).
17. Colley, S., Copperthwaite, R. G., Hutchings, G. J., Loggenberg, P., and Van der Riet, M., *Ind. Eng. Chem. Res.* **27**, 1339 (1988).
18. Colley, S., Copperthwaite, R. G., Hutchings, G. J., Terblanche, S. P., and Thackeray, M. M., *Nature* **339**, 129 (1989).
19. Malats i Riera, A., Pourroy, G., and Poix, P., *J. Mat. Sci. Eng.* **A168**, 245 (1993).
20. Malats i Riera, A., Pourroy, G., and Poix, P., *J. Magn. Mater.* **125**, 125 (1993).
21. Malats i Riera, A., Pourroy, G., and Poix, P., *J. Magn. Mater.* **134**, 195 (1994).
22. Malats i Riera, A., Pourroy, G., and Poix, P., *J. Solid State Chem.* **108**, 362 (1994).
23. Läkamp, S., Malats i Riera, A., Pourroy, G., and Poix, P., *Eur. J. Solid State Inorg. Chem.* **92**, 159 (1995).
24. Pearson, W. B., "Handbook of Lattice Spacing and Structures of Metals." Pergamon Press, 1964.
25. Collongues, R., and Chaudron, G., *C.R. Acad. Sci.* **234**, 728 (1952).
26. Schikorr, G., *Z. Elektrochem.* **36**, 65 (1929).
27. Shipko, F. J., and Douglas, D. L., *J. Phys. Chem.* **60**, 1519 (1956).
28. Schrauzer, G. N., and Guth, T. D., *J. Am. Chem. Soc.* **98**, 3508 (1976).
29. Hindermann, J. P., Hutchings, G. J., and Kiennemann, A., *Catal. Rev.–Sci. Eng.* **35**, 1 (1993).
30. Kiennemann, A., Barama, A., Boujana, S., and Bettahar, M. M., *Appl. Catal.* **99**, 175 (1993).
31. Kiennemann, A., Ernst, B., and Chaumette, P., "Proceedings for the 27th International Symposium Automotive Technololgy and Automation," Aachen, 333 (1994).
32. Chaumette, P., Courty, P., Kiennemann, A., and Ernst, B., *Top. Catal.* **2**, 117 (1995).
33. Kiennemann, A., Boujana, S., Diagne, C., and Chaumette, P., "Proceedings, 10th International Congress on Catalysis, Budapest 1992" (L. Guczi, F. Solymosi, and P. Tetenyi, Eds.), Akadémiai Kidaó, Budapest, 1993.